Asymmetric High-T_c Superconducting Gas Separation Membrane

Eue-Soon Jang,[†] Jae-Joon Chang,[‡] Jihye Gwak,[§] André Ayral,[§] Vincent Rouessac,[§] Louis Cot,[§] Seong-Ju Hwang,[||] and Jin-Ho Choy*[,||]

Emerging Technology Research Department, Advanced Technology Laboratory, Korea Telecom (KT), Seoul 137-792, Korea, School of Chemistry and Molecular Engineering, Seoul National University, Seoul 151-747, Korea, Institut Européen des Membranes, UMR CNRS 5635, CC47, Université Montpellier II, Eugène Bataillon, 34095 Montpellier Cedex 5, France, and Center for Intelligent Nano-Bio Materials (CINBM), Division of Nano Sciences and Department of Chemistry, Ewha Womans University, Seoul 120-750, Korea

Received March 9, 2007. Revised Manuscript Received May 21, 2007

We have developed new asymmetric high-T_c superconducting $(Bi_{1.85}Pb_{0.35})Sr_{1.9}Ca_{2.1}Cu_{3.1}O_{10+\delta}$ membrane with high efficiency for nitrogen separation from air. This membrane with controlled pore structure can be prepared by the electrophoretic deposition of colloidal $(Bi_{1.85}Pb_{0.35})Sr_{1.9}Ca_{2.1}Cu_{3.1}O_{10+\delta}$ nanosheets on the substrate pellet. The presence of mesopores in the asymmetric membrane plays an important role in achieving high gas selectivity through the enhancement of magnetic interaction between the superconductor membrane and oxygen molecules. Also, we have found that the control of experimental factors like the orientation of magnetic field, temperature, and pressure difference across the sample is of special importance in optimizing the gas selectivity of the membrane. The present results underscore the applicability of the superconductor membrane as a gas separation device.

Introduction

Over the past decades, inorganic membranes have attracted intense research interest as alternatives for polymer membranes because of their excellent thermal, chemical, and mechanical stability.[1,2] In principle, the functionality of the inorganic membranes for the purification of mixture is based on their shape and size selectivity. Although limited numbers of successes have been reported for the size-based separation of gas or solvent molecules,[1,2] the inorganic membranes are hardly applicable for the separation of O_2 or N_2 gas from air because of their similar molecular sizes (3.46 Å for O_2 and 3.64 Å for N_2).[3] Instead, the possible separation of nitrogen gas was achieved by the use of the oxide ionic conduction of Bi-based cuprate.[4] However, a high operation temperature (800 °C) of this system may cause serious problems like low durability and high-energy consumption. In this regard, alternative attempts have been made to apply porous high-T_c superconductor (HTSC) membranes for the separation of nitrogen from air.[5] These works are based on the perfect diamagnetic property of HTSC repelling external magnetic field into pores, which prevents the permeation of paramagnetic oxygen molecules through the pores. To date, however, no highly efficient HTSC membrane has been reported for the separation of nitrogen.[6−10] Taking into account the fact that the repelled magnetic flux is concentrated on the pore of the superconductor membrane, a magnetic interaction of the membrane with paramagnetic oxygen molecules would be enhanced by decreasing its pore size.[4,8,9b,11] However, it is not easy to finely tune the pore size of the membrane consisting of microcrystalline HTSC particles. Recently we were successful in synthesizing the colloidal suspension of $Bi_2Sr_2Ca_{n-1}Cu_nO_{2n+4+\delta}$ (n = 1, 2, and 3) superconductor nanosheets with intercalation and exfoliation techniques.[12] The resulting nanosheets were found to be relatively uniform in size with 200 nm in average and high stability in acetone solvent. Their positive surface charge of 25 mV allowed us to apply them to fabricate porous HTSC membrane via electrophoretic deposition.

In the present study, we have fabricated asymmetric porous HTSC membrane of $(Bi_{1.85}Pb_{0.35})Sr_{1.9}Ca_{2.1}Cu_{3.1}O_{10+\delta}$ (hereafter we denote it as (Bi,Pb)2223) by the electrophoretic deposition of the colloidal suspension. The applicability of

* To whom correspondence should be addressed. Tel.: +82-2-3277-4135. Fax: +82-2-3277-4340. E-mail: jhchoy@ewha.ac.kr.
[†] Korea Telecom.
[‡] Seoul National University.
[§] Université Montpellier II.
[||] Ewha Womans University.

(1) Burggraaf, A. J., Cot, L., Eds. *Fundamentals of Inorganic Membrane Science and Technology*; Elsevier: Amsterdam, 1996.
(2) Mulder, M. *Basic Principles of Membrane Technology*, 2nd ed.; Kluwer Academic Publishers: Dordrecht, 1996.
(3) *CRC Handbook of Chemistry and Physics*, 64th ed.; CRC Press: Boca Raton, FL, 1984.
(4) Chen, C.-S.; Liu, W.; Xie, S.; Zhang, G.-G.; Liu, H.; Meng, G.-Y.; Peng, D. K. *Adv. Mater.* **2000**, *12*, 1132.
(5) Reich, S.; Cabasso, I. *Nature* **1989**, *338*, 330.
(6) Sawai, Y.; Bamba, N.; Ishizaki, K.; Hayashi, S. *J. Porous Mater.* **1995**, *2*, 151.
(7) Makarshin, L. L.; Andreev, D. V.; Parmon, V. N. *Chem. Phys. Lett.* **1997**, *266*, 173.
(8) Gordon, R. D.; Cussler, E. L. *Langmuir* **1999**, *15*, 3950.
(9) (a) Yoon, J.-B.; Jang, E.-S.; Kwon, S.-J.; Ayral, A.; Cot, L.; Choy, J.-H. *Bull. Korean Chem. Soc.* **2001**, *22*, 1111. (b) Yoon, J.-B.; Jang, E.-S.; Ayral, A.; Cot, L.; Choy, J.-H. *Bull. Korean Chem. Soc.* **2001**, *22*, 1149.
(10) Gwak, J.; Ayral, A.; Rouessac, V.; Cot, L.; Grenier, J.-C.; Jang, E.-S.; Choy, J.-H. *Mater. Chem. Phys.* **2004**, *84*, 348.
(11) Horie, K.; Ohyagi, M.; Napoli, C.; Ishizaki, K. *Scr. Mater.* **2001**, *44*, 1683.
(12) Choy, J.-H.; Kwon, S.-J.; Hwang, S.-J.; Jang, E.-S. *MRS Bull.* **2000**, *25*, 32.

10.1021/cm070656s CCC: $37.00
Published on Web 06/27/2007

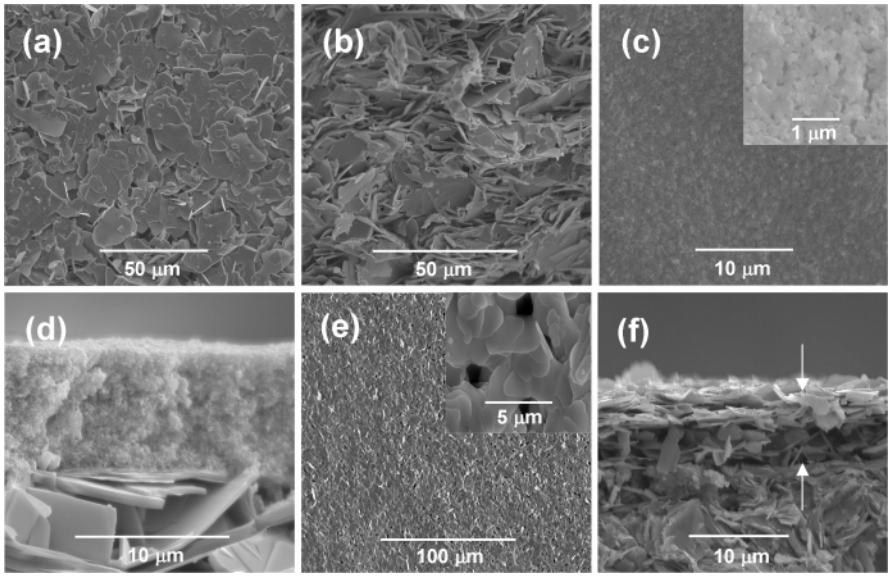

Figure 1. FE-SEM images of the top surface and cross section for (a, b) the (Bi,Pb)2223 substrate pellet, (c, d) the as-deposited asymmetric membrane, and (e, f) the annealed membrane.

the membrane as a gas-separation filter has been systematically investigated as a function of applied gas pressure and the orientation of applied magnetic field.

Experimental Section

Sample Preparation. The substrate pellet of (Bi,Pb)2223 was prepared by high temperature heat-treatment for the pressed precursor pellet of metal oxides and metal carbonates.[13] As a precursor for the colloidal suspension of exfoliated nanosheets, the HgI_2-intercalated (Bi,Pb)2223 was synthesized by stepwise reactions.[13] First, the iodine intercalated (Bi,Pb)2223 compound was obtained by heating the vacuum sealed tube containing the pristine (Bi,Pb)2223 with 5 equiv of iodine per formula unit of host.[11] Then, the intercalation of HgI_2 was carried out by reacting the iodine intercalated (Bi,Pb)2223 and HgI_2 (mole ratio of 1:5) in a Pyrex tube of which the end was opened to air at 253 °C for 24 h. To facilitate HgI_2 intercalation, 1 mol of free iodine as transporting agent was introduced into the tube. The obtained HgI_2 intercalated (Bi,Pb)2223 was subjected to ultrasound with 28 kHz in acetone solvent, leading to the formation of the colloidal suspension of bismuth-based cuprate. All the sonication processes were carried out in an ice bath to protect the samples from overheating. The resulting colloidal suspension was precipitated by a high-speed centrifugation at 15 000 rpm for 30 min. The precipitate was washed with acetone to remove the disintercalated HgI_2 molecules and then redispersed in fresh acetone solvent. The asymmetric porous (Bi,Pb)2223 membrane was fabricated by electrophoretic deposition of colloidal suspension on a 25 mm disk-shaped (Bi,Pb)2223 substrate pellet at 100 V for 5 min, in such a way that both sides of the substrate pellet were deposited by the colloidal particles.

Gas Separation Experiment. In the course of gas separation experiments, a mixture gas (20% O_2 + 80% N_2) was used as feed gas. To prevent the liquidation of oxygen gas (bp 90 K) under a liquid nitrogen temperature of 77 K, air was diluted in helium gas with a volume fraction of 90% determined by mass spectroscopy (MS). The permeate gas was analyzed as a function of pressure gradient across the membrane (ΔP) by gas chromatography (GC). Gas separation experiments for the substrate pellet and asymmetric porous (Bi,Pb)2223 membrane were carried out under the following four different conditions: (1) at room-temperature without external magnetic field, (2) at 77 K without external magnetic field, (3) at 77 K with external magnetic field ($H \perp c$, H = 130 mT) via electromagnet, and (4) at 77 K with external magnetic field ($H \| c$, H = 200 mT) via permanent Nb magnet. In the present experiment, a weaker magnetic field than H_{c1} (650 mT) of the (Bi,Pb)2223 was applied to conserve the perfect diamagnetism without vortex formation. When the external magnetic field was applied to the superconducting membrane, particularly, the sample should be field-cooled (FC) under an applied magnetic field to concentrate the magnetic flux in the pores. If the superconducting membrane was zero-field-cooled (ZFC), the magnetic field will be excluded from the surface of the superconducting membrane, and hence the magnetic flux cannot be concentrated in the pores.

Results and Discussion

FE-SEM Measurement. The morphology of the HTSC membrane has been examined with field-emission scanning electron microscopy (FE-SEM). As illustrated in Figure 1a,b, the substrate pellet of the pristine (Bi,Pb)2223 shows the randomly restacked assembly of microcrystalline plates with the size of ~20 μm. An electrophoretic deposition of the (Bi,Pb)2223 colloidal suspension on the substrate pellet produces uniformly coated layers (thickness ~ 8 μm) consisting of exfoliated nanosheets, indicating the formation of asymmetric HTSC membrane (Figure 1c,d). Because the crystallite thickness of each nanosheet (a few tens of angstrom) is much smaller than the penetration depth of the (Bi,Pb)2223 (λ_{ab} = 250 nm, λ_c = 178 nm),[9,10] we annealed the as-deposited membrane at 850 °C for 6 h to enhance the superconductivity of the coated layer. Upon annealing, the crystallites of exfoliated (Bi,Pb)2223 nanosheets grow up to 6 μm-sized microplates with the formation of sponge-like layers (marked by white arrows in Figure 1f). Also, the annealing at elevated temperature leads to the partial formation of macropores in the deposited top layers (i.e., black holes in the inset of Figure 1e), which would have a detrimental effect on gas separation efficiency. Currently we are trying to tune the annealing condition not only to

(13) Choy, J.-H.; Lee, W.; Hwang, S.-J. *J. Mater. Chem.* **2000**, *10*, 1679.

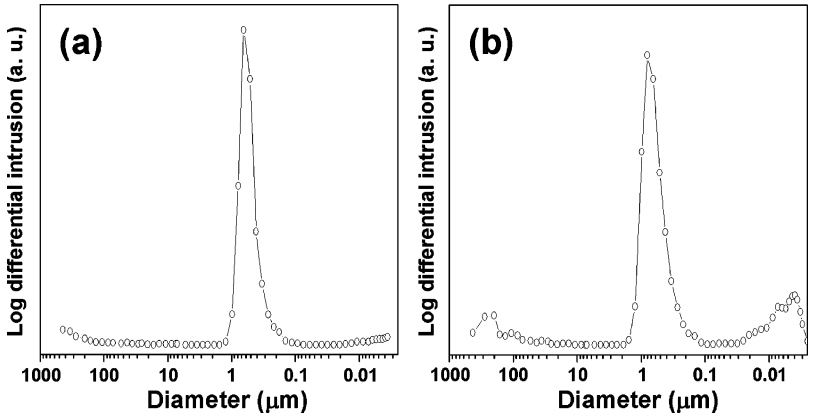

Figure 2. Pore size distribution curves of (a) the substrate pellet and (b) the asymmetric (Bi,Pb)2223 membrane via mercury intrusion method (detection range: 5 nm−10 μm).

minimize the formation of the macropores in the top layer but also to improve the performance of the resultant asymmetric membrane as a gas separation filter.

Pore Size Measurements. The pore size distribution of the substrate pellet and asymmetric membrane of (Bi,Pb)-2223 has been measured with mercury intrusion experiments. Figure 2 represents the pore size distribution curves of the substrate pellet and the asymmetric (Bi,Pb)2223 membrane. The substrate pellet shows the presence of macropores with the average size of 700 nm and the porosity of 24%, indicating that this material is a microfiltration membrane consisting of macropores (>50 nm). After the deposition of the colloidal suspension of (Bi,Pb)2223 nanosheets, the average diameter of macropores and the value of porosity remain unchanged while mesopores with the average diameter of ∼6 nm are newly formed, indicative of the formation of the ultrafiltration membrane. The observed mesopores surely originate from sponge-like (Bi,Pb)2223 layers deposited on the substrate pellet, underscoring the formation of mesoporous sponge-like (Bi,Pb)2223 layers deposited on the substrate pellet. Judging from the pore diameter of each layer, viscous or Poiseuille flow would be developed in the substrate pellet whereas Knudsen flow would be generated in the mesoporous top layers. Because, in the Knudsen diffusion, collisions between gas molecules and the pore wall are more frequent than those between the gas molecules,[1] it is highly feasible that magnetic attractive interaction between the (Bi,Pb)2223 membrane and oxygen would be dominant in the top layer. Moreover, this mesoporous layer with smaller pore size is more effective in concentrating magnetic flux on the inside of pores compared to the macroporous substrate.

dc Magnetization Measurement. The superconductivity of the substrate pellet and the membrane was examined by measuring the ZFC direct current (dc) magnetizations as a function of temperature. As presented in Figure 3, both the samples were distinctively superconducting with a T_c of 108 K without any appearance of secondary onset due to the formation of impurity phases. Also, both the materials unfold nearly identical values of diamagnetic signals of −0.08 emu/g at 77 K, corresponding to the superconducting shielding fraction of ∼80%.

Permeation Measurements. We have examined the permeation of air (10%)−He (90%) gas mixtures as a

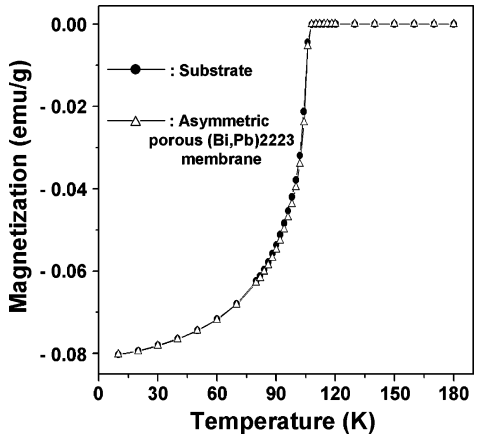

Figure 3. Temperature-dependent curves of ZFC dc magnetization for the substrate pellet (circles) and asymmetric porous (Bi,Pb)2223 membrane (triangles).

function of pressure difference (ΔP) across the samples. The permeances of the substrate pellet and the asymmetric porous (Bi,Pb)2223 membrane are plotted in Figure 4 as a function of pressure difference across the sample. The permeance of the substrate pellet becomes larger as the ΔP increases from 0.1 to 1.0 bar but decreases as the temperature increases from 25 to 80 °C, indicating that gas transport through the macroporous substrate corresponds to viscous flow.[1,2] On the other hand, the asymmetric (Bi,Pb)2223 membrane shows similar dependency of permeance on ΔP and temperature to the substrate. However, the permeance values and their slope against ΔP are much smaller than those of the substrate. This can be regarded as an evidence of the Knudsen flow in this material due to the presence of the mesoporous top layers.[1,2]

Figure 5 shows the gas selectivity (α_{N_2/O_2}) of the substrate pellet and asymmetric (Bi,Pb)2223 membrane as a function of pressure difference (ΔP) across the samples. The selective permeances of gas molecules were measured under the control of experimental conditions like the strength and orientation of applied magnetic fields and measurement temperature. Gas selectivity (α_{N_2/O_2}) can be calculated as the following equation:[10]

$$\alpha_{N_2/O_2} = \frac{N_2(\text{permeate})/N_2(\text{feed})}{O_2(\text{permeate})/O_2(\text{feed})} \quad (1)$$

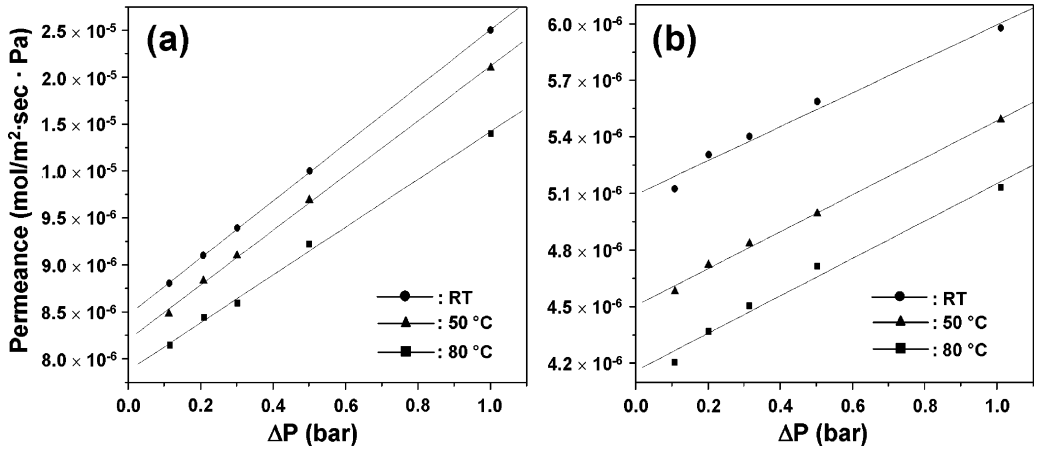

Figure 4. Permeances of (a) the substrate pellet and (b) the asymmetric porous (Bi,Pb)2223 membrane as a function of pressure difference across the sample.

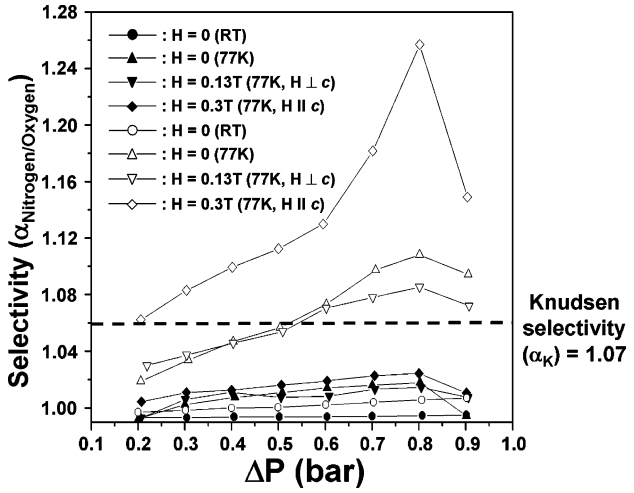

Figure 5. Gas selectivity (α_{N_2/O_2}) of the substrate pellet (closed symbols) and asymmetric (Bi,Pb)2223 membrane (open symbols) as a function of pressure difference (ΔP) across the samples. The dashed line represents theoretically calculated Knudsen selectivity ($\alpha_K = 1.07$).

For the substrate pellet, the gas selectivity remains close to unity for all the present experimental conditions, strongly suggesting that magnetic interaction in this material is too weak to trap oxygen molecules. Such a poor selectivity of the macroporous HTSC pellet was already reported for (Bi,Pb)2223 and $YBa_2Cu_3O_{7-\delta}$.[8] To overcome such a drawback, we came up with an idea that the asymmetric (Bi,Pb)-2223 membrane under investigation would exhibit a marked dependence of gas selectivity on the orientation of magnetic field and measurement temperature. While the room-temperature data without magnetic field represent no marked enhancement of α_{N_2/O_2} value from unity, the lowering of the temperature to 77 K distinctly increases the gas selectivity above the value of the Knudsen selectivity ($\alpha_K = 1.07$) for high ΔP region. Similar degree of selectivity increase can be induced by the application of magnetic field along the $H \perp c$ direction. Of special interest is that the application of magnetic field parallel to the *c*-axis of the membrane remarkably enhances the gas selectivity to 1.26 at $\Delta P = 0.8$ (Figure 5), as expected.

The observed remarkable dependence of gas selectivity on the field orientation can be understood as follows. As illustrated in the schematic diagrams of Figure 6a, the magnetic flux applied perpendicularly to the *c*-axis of the (Bi,Pb)2223 membrane passes along the *ab*-plane of membrane, leading to the negligible trapping of the magnetic flux on the pores. On the contrary, the application of magnetic field oriented parallel to the *c*-axis gives rise to an effective concentration of magnetic flux on the pores of the HTSC membrane; see Figure 6b. In this case, significant field gradient (dH/dx) is created in the cavity of the (Bi,Pb)2223 membrane, leading to the trapping of paramagnetic oxygen molecules.

A magnetic force F between applied magnetic field and particle can be expressed as the following equation:[6,9b]

$$F = M\frac{dH}{dx} = \frac{M}{\mu_0}\frac{dB}{dx} = \frac{\chi_m}{{\mu_0}^2}B\frac{dB}{dx} \qquad (2)$$

where M is the induced magnetization of a particle, χ_m is the magnetic susceptibility, H is the applied field intensity, B is the induced magnetic field intensity, dB/dx is the magnetic field gradient, and μ_0 is the magnetic permeability of a vacuum. On the basis of this equation, the magnetic force F is expected to be larger for the mesopores with larger dB/dx than for the macropores with smaller dB/dx. Hence, paramagnetic oxygen molecules can be effectively trapped in the mesopores of the top layer under parallel-aligned magnetic field ($H \| c$), verifying the usefulness of the formation of the asymmetric membrane. In contrast, diamagnetic nitrogen molecules can pass through the membrane without any influence of the magnetic field.

On the other hand, all of the present selectivity data show similar pressure dependences, in which the increase of ΔP results in the improvement of selectivity in the ΔP region of 0.2−0.8 but depresses the selectivity beyond an optimum condition ($\Delta P = 0.8$). The observed improvement of selectivity with respect to ΔP in the low-pressure region is contrasted with the expectation that attractive interactions between oxygen molecules and magnetic flux would be enhanced at low ΔP condition. However, in the high-pressure region, the condensation and liquidation of oxygen molecules diluted in He gas are expected to frequently occur. It has been well-known that the magnetic susceptibility (χ_m) of liquid oxygen (7.67×10^{-9} m^3/mol) is larger than that of gaseous oxygen (3.40×10^{-9} m^3/mol).[9b] Hence, an attractive

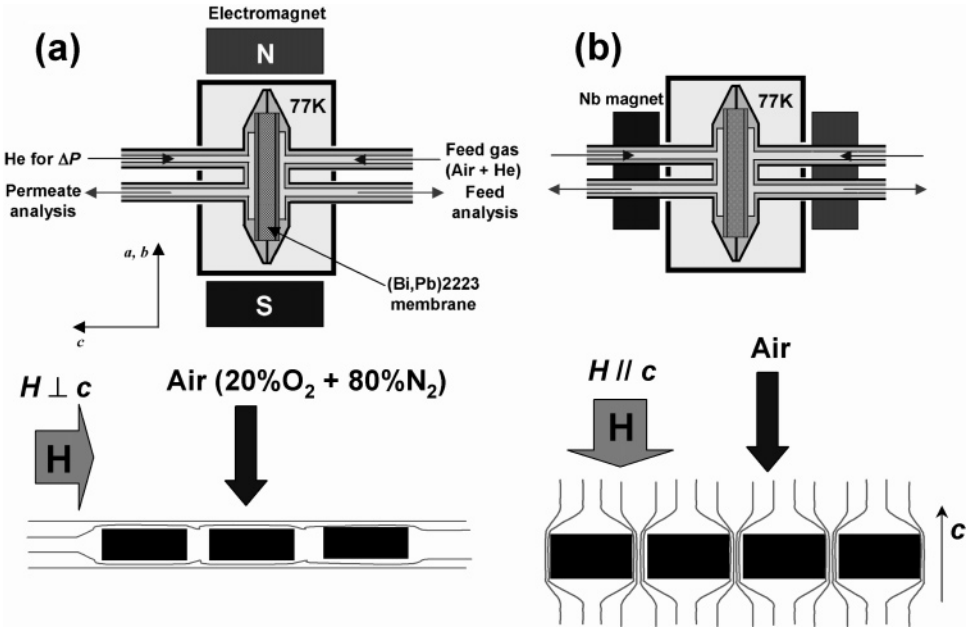

Figure 6. Schematic representations of the orientation effect of magnetic fields on the concentration of fluxes inside the pores: (a) $H \perp c$ and (b) $H \| c$.

force F becomes increased through the condensation of oxygen molecules. This phase change allows us to explain the observed increase of selectivity with ΔP at lower pressure region. Also, we are able to attribute the depression of selectivity beyond the optimum pressure ($\Delta P = 0.8$ bar) to the enhanced escape of trapped oxygen, because in this region the kinetic energy of gas molecules would prevail over the magnetic interaction with the HTSC membrane.

In summary, we are successful in developing the asymmetric (Bi,Pb)2223 membrane with high efficiency for nitrogen separation from air. This membrane with controlled pore structure can be prepared by the electrophoretic deposition of colloidal (Bi,Pb)2223 nanosheets on the substrate pellet. The presence of mesopores in the asymmetric membrane plays an important role in achieving high gas selectivity through an enhancement of magnetic interaction between HTSC membrane and oxygen. In addition, we have found that the control of experimental factors like the orientation of magnetic field, temperature, and pressure difference across the sample is of special importance in optimizing the gas selectivity of the membrane.

Acknowledgment. This work is financially supported by the Science and Technology Amicable Research (STAR program) and partly by the SRC/ERC program of MOST/KOSEF (Grant R11-2005-008-01001-0).

CM070656S